The fluid dynamics of yellow dung fly sperm flow

Christian Wüst [a,b], S.A.Sauter [b], P.I.Ward [a], L.F.Bussiere [a,c]

Zoological Museum, Unversity of Zurich [a]
Institute of mathematics, Unversity of Zurich [b]
School of Biological and Environmental Sciences, University of Stirling [c]

Abstract

The mechanisms regulating sperm transfer, storage, and use in insects are far from clear. Even in one of the most well-resolved systems for studying post-copulatory sexual selection, the yellow dung fly (*Scathophaga stercoraria*), the process of sperm transfer is not well understood. Our aim is to model the fluid dynamics of sperm flow in the reproductive tracts of female yellow dung flies to determine what aspects of female morphology may influence sperm movement. We model fluid flow using computational mathematics, and investigate geometric parameters suspected of influencing rates of ejaculate movement: the curvature of sperm storage ducts, the smoothness of the inner duct wall (surface area), spermathecal duct length and duct diameter. Duct length does not influence the flow rate, where duct diameter has a strong influence of up to 71% at the extremes of the natural range observed in female dung flies. Whereas duct curvature influences the flow rate only slightly (with an effect size of 1.6% over the natural range), the duct wall smoothness has a pronounced effect (50%). The increase in duct surface area also slightly increases the effect of curvature, implying that these structures might act synergistically, although the small size of this effect argues against such a synergy having evolved as an adaptation for controlling sperm flow. We discuss the implications of our model and methods for research in sperm competition and sexual selection.

Key words: Scatophaga stercoraria, sperm competition, spermathecae, stokes flow, finite elements
PACS:

1. Sperm displacement in yellow dung flies

The recognition that sexual selection continues after mating has initiated tremendous research on the mechanisms and consequences of sperm competition (the competition between sperm for the fertilization of ova, Parker (1970a) and cryptic female choice (any female-controlled trait or process that influences the outcome of sperm competition, Eberhard (1996)). In spite of this research focus, the evolutionary consequences of postcopulatory sexual selection remain poorly resolved. This is partly because, unlike premating sexual selection, many of the crucial events are concealed within the reproductive tracts of females and therefore less amenable to direct observation and manipulation. In addition, postcopulatory sexual selection involves several individuals (i.e., a female and at least two competing males), each of which may have multiple interests in the outcome of selection that may or may not be congruent with the interests of the others. These competing interests interact in complex ways, and there are numerous examples of manipulative interactions in which behaviours or structures in one individual have come about in part via manipulation by another individual (Arnqvist, 2005; Blanckenhorn et al., 2007). As a consequence, disentangling the selective basis and functional sig-

nificance of traits that may have evolved in the context of postcopulatory sexual selection is difficult, even in very well studied systems.

The yellow dung fly (*Scathophaga stercoraria*) is a model system for research on post-copulatory sexual selection since the early 1970s (Parker, 1970a,b). Males congregate on dung pats to which gravid females are attracted for the purpose of oviposition (Parker, 1970b), and compete to copulate with these females. Although females do not appear to have any significant control over the identity of their mates at the oviposition resource (Parker, 1970a,b), they do seem to retain some degree of control over insemination (Hosken et al., 2001). Females do assist sperm movement from the intromittent organs to the primary site of sperm storage, as evidenced by experiments featuring female anesthesia (Bernasconi and Hellriegel, 2002) and radiolabelling techniques (Simmons et al., 1999). More intriguingly, females appear to be able to sort sperm in their multiple sperm storage organs (Bussière et al, unpublished, Demont et al, unpublished) perhaps in order to manipulate the paternity of their offfspring depending on the predicted environmental conditions larvae will face (Ward, 2000, 2007).

Although there is strong selection on males to achieve insemination success, (Parker, 1970a; Parker and Simmons, 1991; Simmons and Parker, 1992; Parker and Simmons, 1994; Simmons et al., 1999), there is nevertheless considerable variation in the relationship between male traits and success in paternity (Simmons and Siva-Jothy, 1998). Such variation might be partly attributable to female adaptations designed to retain control over sperm movement (Hosken et al., 1999; Arthur et al., 2008). For example, Hosken et al. (1999) have suggested that the convoluted nature of the spermathecal ducts may serve to restrict sperm movement to the spermathecae and thus assist female control over insemination succcess. Similarly, the curvature of ducts, acting in concert with the spermathecal invagination (Hosken and Ward, 2000) may play a prominent role in female mediated sperm transport. Documenting the role of putative adaptations for controlling sperm flow is made difficult both by the small scale of the structures involved and by the potential interactions between males and females that might influence the outcome of sexual interactions. In this manuscript we use computational mathematics to examine the potential for female anatomy to affect the flow of ejaculates through spermathecal ducts. Our aim is to identify those structures that are most likely to influence flow rates as targets of further empirical investigation on the role of females in controlling insemination.

2. The role of the female in sperm displacement

There is some evidence that female characters in general, and the morphology of the reproductive tract specifically, may affect the outcome of post-copulatory sexual selection by biasing the success of different males in reaching the sites of insemination and fertilization (Minder et al., 2005; Miller and Pitnick, 2002).

The reproductive tract of the yellow dung fly female is a complex collection of organs. Sperm are transferred from the male aedeagus into a muscular bursa copulatrix, and move from there to the sperm storage organs, known as spermathecae (Fig. 1). There are usually three (rarely four, Ward (2000)) spermathecae arranged into a singlet on one side of the body and two spermathecae collectively called the doublet on the opposite side. Each spermatheca has its own independent narrow duct through which sperm must travel to and from the site of sperm storage (Hosken et al., 1999).

The duct entrances at the bursa are all close to each other, and the spermathecal ducts are lined internally with chitin that forms circular ridges around the circumference of the ducts. This inner lining is extremely irregular because it is lined with microvilli (a characteristic which we will refer

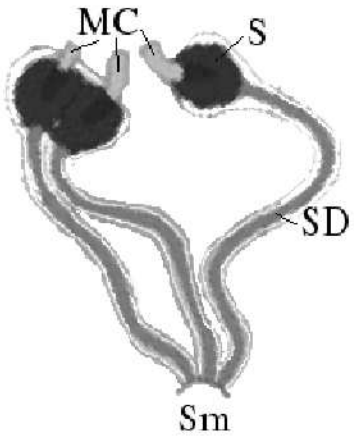

Fig. 1. *Scathophaga stercoraria*, detail of the female genital tract (redrawn from Arthur et al. (2008)). S, spermatheca; SD, spermathecal duct; Sm, spermoraria; MC, muscular copulatrix.

to as the duct's internal surface area), especially compared to the lining in the spermathecae (fig. 2) (Hosken et al., 1999). We will compare fluid flow in ducts lined with microvilli to ducts of the same width that lack these structures.
The ducts are surrounded by longitudinal muscle and are $672 \pm 17\mu m$ long. The width of the ducts are $13.5 \pm 1.8\mu m$ excluding the microvillosity which has a dimension of around $1 - 2\mu m$ (Hosken et al. (1999)).

Another putative adaptation may be the degree

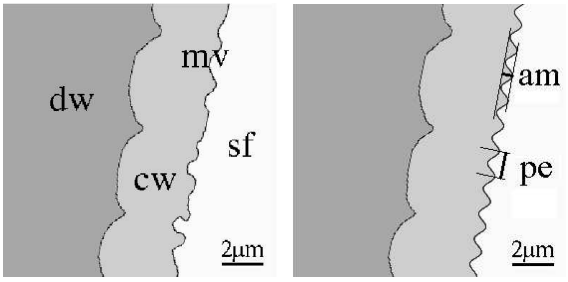

Fig. 2. *Scathophaga stercoraria*, left: detail of the spermathecal duct wall redrawn from (Hosken et al., 1999). cw chitinous wall, dw, duct wall; mv, microvilli (increased surface area); sf, seminal fluid. right: detail of the increased surface area as modelled by sine waves for the purpose of studying their effects on fluid dynamics. am, aplitude of the mv; pe, period of the mv.

of curvature exhibited by ducts. Because of the musculature associated with ducts and observable in live preparations, such an adaptation could provide females with more plasticity in their response to different males if curved ducts slow the rate of fluid flow. For example, by tightening the muscle attached to the spermathecal invagination, females could straighten the duct and allow more rapid sperm flow relative to the situation in a curved duct (which is the natural resting state).

3. Assumptions and simplifications of the model

The physical, mathematical and numerical modelling of sperm flow is an emerging field in computational biology which is far from being fully understood. In this paper, we will develop a numerical solution method for a two-dimensional model which may clarify the possible role of some female reproductive structures in affecting the movement of seminal fluid. The concept of the model, the methods and their implementation is designed such that more advanced models and/or advanced numerical methods can be realized in a modular way in the future. In the following list we describe the model assumptions and discuss their generality.

(i) The system is considered stationary (no time dependence) and inertialess (Stokes flow, see next section).

(ii) The equation system for the fluid flow is solved on a discrete mesh of around 10^5 degrees of freedom (see next section).

(iii) The increased surface area is modelled using sine waves to simulate duct wall complexity (Figure 2). Mathematically, this is a straightforward parameterization of irregular boundaries.

(iv) The model is two dimensional (see next section).

(v) The physical quantities: We can reasonably bound the order of all the quantities used (Table 1).
Density and *viscosity* are estimated based on properties of body fluids from other species of insects. For example, in *Manduca sexta*, the hemolymph is estimated to have a density of between 1-10 centiPoise (D. Saunders, pers. comm.).
The *inflow velocity* is estimated from the fact that it takes less than 5 minutes for sperm to reach the spermathecae after the onset of copulation (Hosken et al., 1999). In the discussion we analyse the sensitivity of each of these parameters to the outcome of our tests.

Model parameter	Estimated quantity
density (ρ)	$1g/cm^3$
dynamic viscosity (μ)	$0.1poise$
kinematic viscosity (ν)	$10^7 \mu m^2/s$
inflow velocity (U)	$2\mu m/s$

Table 1
Estimated physical quantities for dung fly seminal fluid. The values are either deduced from other species or approximated by measurements described in section 3

(vi) The duct is modelled as a pipe with inflow and outflow. The inflow is given as a velocity profile along the inflow edge. The outflowing fluid has zero parallel component to the outflow edge:

$$u = u_{parabolic} \text{ on } \Gamma_{\text{inflow}}, \quad u \cdot \tau = 0 \text{ on } \Gamma_{\text{outflow}}, \tag{1}$$

where $u_{parabolic}$ is the given velocity described in the next section and τ a unit vector perpen-

dicular to the outflow edge. These are *boundary conditions* for the mathematical description of the model (see next section).

(vii) The fluid containing the sperm filaments is modelled as a *homogeneous fluid* with homogenous material properties.

The last two assumptions are considered more fully in the discussion.

4. Modelling sperm flow

In fluid dynamics there are two characteristic flow regimes: *laminar* and *turbulent flow*. *Laminar flow* means smooth flow in parallel layers (e.g. pressing tooth paste out of the tube) where *turbulent flow* always includes vortices and chaotic, stochastic property changes (e.g. water flow around a ship). To distinguish those two regimes we introduce the dimensionless *Reynolds number*:

$$\mathrm{Re} := \frac{L \cdot U}{\nu}, \tag{2}$$

where L is a characteristic length, U a characteristic velocity and ν the kinematic viscosity of the system. Laminar flows have a Reynolds number smaller than 2300 and turbulent flows larger than 2300. For more details see Batchelor (1967).

Flows at very small scales are typically strongly laminar. Since we cannot measure most of the quantities needed, we must estimate them. According to the estimates in Table 1 the Reynolds number of the system is 10^{-7} for the sperm flow inside the duct of the female yellow dung fly. We direct readers to Purcell's review Purcell (1977) of flow at low Reynolds numbers for more information on strongly laminar flow.

Briefly, sperm flow in yellow dung fly females behaves like viscous layers. Although the *fluid* is not viscous ($\nu_{\text{fly sperm}} \approx \nu_{\text{olive oil}}$), the *flow* is viscous: If the system were scaled up to a magnitude in which the ducts width was $1cm$, the flow would be even more viscous than honey pouring through the tubes. This makes the construction of a scaled-up model for experimental validation very difficult: most fluids that are sufficiently viscous at a reasonable domain size possess inappropriate properties. Considering mathematical modelling, strongly laminar flow (Stokes flow) of homogeneous fluids is well understood in this context.

Under the given assumptions, derived from the physical laws conservation of mass and momentum, laminar flow can be described by the dimensionless *Stokes equations*

$$\begin{aligned} -\frac{\partial^2 u_1}{\partial^2 x} - \frac{\partial^2 u_1}{\partial^2 y} + \frac{\partial p}{\partial x} &= 0 \\ -\frac{\partial^2 u_2}{\partial^2 x} - \frac{\partial^2 u_2}{\partial^2 y} + \frac{\partial p}{\partial y} &= 0 \quad \text{in } \Omega \\ \frac{\partial u_1}{\partial x} + \frac{\partial u_2}{\partial y} &= 0 \\ &+\text{boundary conditions,} \end{aligned} \tag{3}$$

where (x, y) are the spacial coordinates, $\mathbf{u}(\mathbf{x}, \mathbf{y}) = (u_1(x, y), u_2(x, y))$ is the fluid velocity and $p(x, y)$ is the pressure in (x, y).

The first equation represents the conservation of momentum (continuity equation), and the second equation represents the conservation of mass. The boundary condition describes the behavior of the fluid at the boundary and completes the system to have a unique solution in appropriate function spaces.

Given the fluid properties, the boundary conditions (such as in- and outflow) and the two-dimensional morphology of the duct, we can calculate the velocity and the pressure of the fluid in the given domain using the Stokes equations. Solving these equations presents mathematical and computational challenges. Although dealing with laminar flow is much easier than dealing with turbulent flow, one is in general unable to analytically find the exact solution of the Stokes equations. Therefore there are numerous *numerical methods* to find a good approximation of the solution.

We use the *finite element method* (Girault and Raviart, 1979; Ciarlet, 1978; Hackbusch, 1992). The main idea behind this method is to subdivide the domain (the spermathecal duct) in a finite number of very small subdomains called elements. In two dimensions we use triangles as elements. Based on this *finite element mesh* we construct the *finite element space*. The method leads to a system of linear equations, the solution to which yields an approximation of the exact solution. Finer grids (more elements) produce better solutions, and as the *mesh width* approaches zero, the approximation approaches the continuous solution. Accordingly, one would like to have as many elements as possible to approximate the true solution. The limiting factor is determined by the memory and speed of the computer and the programming language architecture. The most demanding task for the computer is to solve the arising linear system. Solving

the problem (especially modelling flow around microstructures) in three dimensions require complex numerical techniques. Developing such methods is an emerging field in computational mathematics.
For the investigation we use two-dimensional finite elements which sacrifice some realism, but by using state-of-the-art finite element technology it is possible to discretize the spermathecal duct in two dimensions by $10^5 - 10^7$ elements.
Fluid flow in small tubes (*Poiseuille flow*) is well understood (Lighthill, 1975), and a way of finding the exact solutions for the Stokes problem in straight pipes is shown in the next section. This allows us to verify the mathematical model and use it for our more complicated, curved ducts.

5. Stationary circular pipe flow

In this section we will derive the exact solution (u, p) for a simple model problem.
Consider a straight (for now infinitely long) two-dimensional pipe with the y-axis as its axisymmetrical center and radius a. We use a Cartesian coordinate system and consider stationary flow. Note that the flow field is constant with respect to the axial component y since the pipe is infinitely long.
The continuity equation yields $u_1 = 0$ in the whole pipe. This means there is no movement in the radial direction. Considering the radial component of the momentum equation, it follows that the pressure p is constant across the cross-section of the pipe. Moreover, using the axial component of the momentum equation, we find that the pressure gradient $\partial p/\partial y$ is constant. Finally we have simplified the momentum equation to

$$\left(\frac{\partial^2 u_2}{\partial^2 x} + \frac{\partial^2 u_2}{\partial^2 y}\right) = \frac{\partial}{\partial y} p = \text{constant}. \tag{4}$$

This equation can be solved analytically, and by enforcing the *no-slip* boundary condition (the fluid at the wall cannot move) we get

$$u_2(\mathbf{x}) = c_1 \frac{\partial p}{\partial y}\left(x^2 - a^2\right), \tag{5}$$

where $c_1 := 1/2$. This is the *Poiseuille flow*. The formula shows that the axial flow profile is parabolic with a maximum at the centerline. Further, the flow velocity is proportional to the pressure gradient $\partial p/\partial y$.
An important quantity of our tests is the flow rate $\dot{Q}$ which describes how much fluid is transported through a cross section per second. Mathematically

$$\dot{Q} = -c_2 a^3 \frac{\partial p}{\partial y}, \tag{6}$$

where $c_2 := 2/3$. This is known as *Poiseuille's law*. Using Poiseuille's law we can compute the pressure drop along a finite canal of length L with centerline velocity U_0. Combining (5) with (6) and the shape of the inflow function, we find that

$$\dot{Q} = \frac{c_2}{c_1} a \pi U_0 \tag{7}$$

and obtain for the pressure drop due to the linearity of p

$$p(L) - p(0) = L\frac{\partial p}{\partial y} = -L\frac{c_1 U_0}{a^2}. \tag{8}$$

Thus, we derived an exact solution for the infinitely long straight pipe. However, the spermathecal ducts are of finite length and curved. For pipes of finite length we can no longer give a general exact solution since the flow in the entry region is, in general, not the same as the one in the infinitely long pipe. There are methods to approximate the flow in the entry region. They indicate that in flows of low Reynolds numbers the region affected by irregularities near the entry is shorter than in flows of higher Reynolds numbers. Therefore we ignore this effect. As a validation we use in our tests an exact inflow according to (5) to compare the numerical approximations with the exact solution in (8).
We cannot give an exact solution for flow in curved pipes either. Its analysis relies strongly on numerical and physical experiments by (Dean, 1927, 1928). These special curvature effects (centrifugal effects, vortices) can also be directly related to the Reynolds number. More precisely, the *Dean number*

$$\mathrm{De} := \mathrm{Re}\sqrt{\frac{\text{pipe radius}}{\text{centerline curvature radius}}}$$

is a measure for these effects. Since the Reynolds number is very small in our application, we also have $\mathrm{De} \ll 1$. Therefore these irregular flow effects in curved parts of the duct can be neglected. Nevertheless, fluid flow in curved tubes is affected more by friction at the wall of the duct. For our numerical experiments we therefore expect a slightly smaller flow rate in more curved tubes.

6. Methods and computer simulations

We implemented the numerical algorithm to model the flow problems using computational mathematics. The strength of the software we created

is its generality. The investigator can trace reproductive tract structures from micrographs or draw a domain of arbitrary design in the computer. In addition, one can run two tests that are identical with the exception of a single parameter (e.g. the curvature of the duct) in order to evaluate the effect of a given parameter on fluid flow.
Once one has fixed the settings, the program yields an approximation to the solution of the described problem. The parts of the calculations that are costly in terms of time are parallelized using the shared-memory technique, e.g. we solve the equation system using PARDISO (Schenk and Gärtner, 2004, 2006).

7. Numerical Experiments

In this test series we set up experiments to determine the influence of several morphological parameters. We will compare these results qualitatively with those for the analytically completed solutions of the Poiseuille flow.
For each parameter we consider how the results would differ for a three-dimensional model relative to our own.

Flow rate dependance on a change in duct length

Changing the *length* of a duct will not change the flow rate since the pressure drop remains constant at the same value. Nevertheless it will take each particle longer to cross the whole duct. Using our seminal fluid velocity estimate, it takes a single sperm less than 5 minutes, meaning a minimum rate of travel of $2\mu m/s$. Using this minimum flow rate, we can estimate that if duct was $700\mu m$ rather than $600\mu m$, sperm transport would require 30 seconds more from the duct entrance to the spermatheca.

Flow rate dependance on a change in duct diameter

A change in the *diameter* of a straight duct will produce a change in the flow rate. Equation (7) shows a linear relationship between flow rate and duct radius in two dimensions, whereas in three dimensions the relation is quadratic. Using a range of $d = 13.5 \pm 1.5\mu m$ we find that the flow rate at $d = 12\mu m$ is ≈ 0.75 times the flow rate at $d = 13.5\mu m$, whereas the flow rate is ≈ 1.28 times larger at a diameter of $d = 15\mu m$. Comparing the extreme diameters, the flow rate is $\approx 71\%$ larger at $d = 15\mu m$ than at $d = 12\mu m$.

For the following tests we fix the following parameters in order to assess the influence of the reproductive tract curvature and roughness. We model a spermathecal duct $600\mu m$ long with a diameter of $13.5\mu m$. We specify the inflow as from the exact solution of (5) and choose the centerline velocity $U_0 = 4\mu m/s$, which is equivalent to a mean inflow speed of $(8/3)\ \mu m/s$.
The resulting quantity of the computational tests is the pressure drop in the inflow versus the outflow. Comparing two calculations for the same diameter, length and inflow, the flow rate is reciprocally proportional to the pressure drop. If the flow encounters double the pressure loss, then, at the same force pressing the fluid into the tube, only half of the fluid would flow through in the same time.

Effect of increased surface area in a straight duct

The increased surface area is modelled by superimposing an oscillating sine function (Figure 2). We chose sine *period* values of $1, 1.5$ and $2\mu m$. For each of these values sine *amplitudes* of $0, 0.5, 1, 1.5$ and $2\mu m$ were tested. The mean values for this range were suggested by Hosken et al. (1999). For these 15 combined test-cases the pressure drop is shown plotted against the amplitude in Figure 3. For every sine wave it is obvious that

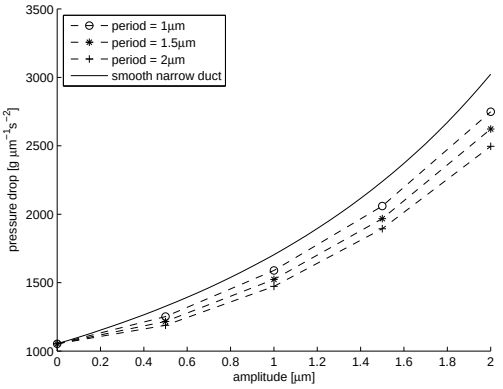

Fig. 3. Pressure drop versus increased surface area amplitude for different periods compared with the *smooth narrow duct*. Since pressure drop $\approx 1/$(flow rate) it shows the effect of curvature on the flow rate (higher values mean less flow).

the case with an amplitude of 0 (the duct with a smooth boundary) is a lower bound. As an upper bound we consider the same smooth duct but with a

reduced diameter as small as the minimal diameter of the duct with increased surface area (diameter $d - 2 * amp$). We call this parameter set *smooth narrowed duct* in Figure 3.
For a fixed amplitude the pressure drop increases as the period decreases towards the value of the narrow duct. For a fixed period the pressure drop can be accurately fitted with a quadratic function.
For a moderate level of surface area (amplitude = 0.5 and period = 1.5) the pressure drop is scaled by a factor of about 1.15 compared to the smooth duct. Since the increased surface area is a radial parameter (the effect acts in three dimensions, even though the model is limited to 2-D), it has a quadratic effect on the flow rate in three dimensions (7). The flow rate is estimated to be more than halved (factor 1/2.25) when applying a moderate amount of duct roughness in three dimensions.

Effect of curvature in a smooth walled duct with a constant total length

The model of a curved duct is chosen as follows: We divide the centerline of the straight duct into three parts. Each part is then modelled using a Bezier curve of order 2. The total length is fixed at $600\mu m$. The curvature is parameterized by the bottom left angle α of the artificial Bezier line (Figure 4). From the resulting smooth curve the duct

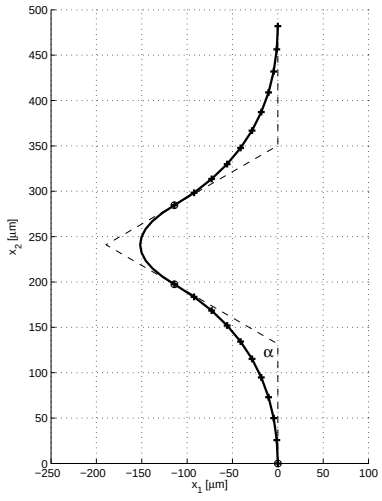

Fig. 4. The curved duct centerline with parameter α of length $600\mu m$.

boundary is obtained simply by orthogonal outward projection of the centerline. We limited the angles studied by measuring photographs of duct curvature angles for natural female reproductive tracts. The range we use represents the range of natural angles for these ducts

$$\alpha \in \{125, 130, ..., 180\},$$

where $\alpha = 180$ is the straight duct (for which the exact solution is already known).
For four different duct diameters, the computed data is shown in Figure 5. The relative pressure drop increments from $\alpha = 180$ to $\alpha = 125$ are presented in Table 2. Since the increment for $d = 13.5\mu m$ is only about 1.6%, we see that curvature does not substantially affect the flow. However, as predicted in the end of section 5, there is a larger pressure loss at more acute angles (representing more curvature).
Using the exact solution for $\alpha = 180$ and a quadratic

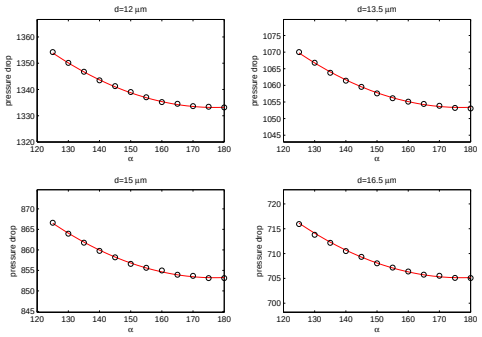

Fig. 5. Pressure drop versus curvature parameter α for different duct diameters. The circles denote the computed results and the line denotes the function δp_{fit}. Since pressure drop $\approx 1/$(flow rate) it shows the effect of curvature on the flow rate (higher values mean less flow).

Spermathecal duct diameter	Pressure drop increment in %
$12\mu m$	1.580
$13.5\mu m$	1.610
$15\mu m$	1.580
$16.5\mu m$	1.542

Table 2
Percentage pressure drop from $\alpha = 180$ to $\alpha = 125$. Since pressure drop $\approx 1/$(flow rate) it describes the effect of curvature on the flow rate.

fit obtained from the computational results, we derive the following approximation:

$$\begin{aligned}\delta p_{fit} &:= (p_{in} - p_{out})(a, \alpha) \\ &\approx \frac{48000}{a^2} \\ &\quad * \left(5.754 * 10^{-6}\alpha^2 - 2.037 * 10^{-3}\alpha + 1.180\right)\end{aligned} \tag{9}$$

The quadratic coefficient in (9) is small, hence the function is nearly linear. Using a cubic fit produces a cubic coefficient of the order 10^{-9}. This means that the pressure drop depends quadratically on the angle α. Equation (9) shows also that at fixed angle α the pressure drop depends on $1/a^2$. This leads to a linear relationship between flow rate and diameter in curved ducts (as shown in (7)).
These results are transferable to the three-dimensional case since the curvature of ducts occurs primarily in one dimension.

Effect of curvature on flow in a duct with moderate microvillosity

As seen in the previous two tests, a rough surface affected the fluid flow by about 50% whereas the bending of the duct only resulted in a difference of about 1.5%. Now we will study these two parameters simultaneously. We add a moderate surface area to the same model of curvature. We test the two cases $period = 1.5/amplitude = 1$ and $period = 1.5/amplitude = 0.5$. These values are obtained by measurements from micrographs of spermathecal ultrastructure (Hosken et al., 1999).
The behaviour illustrated in figure 6 is approximately the same as that in figure 5. The drop in pressure reacts quadratically to a decrease in the angle of curvature α. As in Figure 3, the amplitude of the surface area has the largest influence on the fluid flow. In contrast, the curvature affects the flow only slightly; for an amplitude of $0.5\mu m$ the effect is only 1.7%, and for an amplitude of $1\mu m$ it is only 1.8%. The increase in surface area has slightly increased the effect of curvature.

8. Discussion

Natural levels of curvature influence the flow rate only slightly (with an effect size of 1.6%) whereas increasing the surface area has a pronounced effect (50%). The increased surface area of ducts that is a product of microvilli slightly augments the effect of curvature, implying that these structures might act synergistically, althought the combined effect is only slightly larger than that caused by microvilli alone.

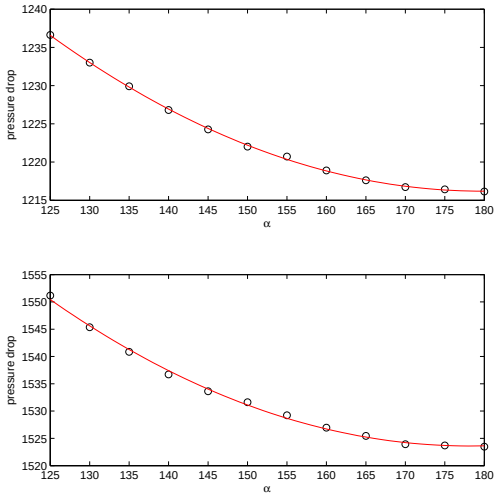

Fig. 6. Pressure drop versus curvature parameter α where $period = 1.5, amplitude = 1$ and $period = 1.5, amplitude = 0.5$. The lines are quadratic fits for the measured data. Since pressure drop $\approx 1/$(flow rate) it shows the effect of curvature with increased surface area on the flow rate (higher values mean less flow).

Due to the laminar behaviour of fluids in our system, a restricted duct diameter has a similar and slightly larger impact on flow rate as increased surface area. The length of the duct has no influence on the flow rate but does influence the time required for sperm to move into the storage organs.
As mentioned in section 3, we address the last two assumptions.

Boundary condition setting: given inflow, parallel outflow

This assumption is a simplification of the real situation that we do not yet understand: flow may not be constant because it may occur in both directions (Simmons et al., 1999). The outflowing seminal fluid is collected in the spermathecae, which gradually become full, and there may be an accumulation or obstruction caused by the finite volume of the sperm storage organs. We are thus limited in our tests, but being aware of these simplifications we can nonetheless model the effect of morphology on flow rate, especially in virgin flies with empty spermathecae.

The fluid is homogeneous

Mechanics of flexible bodies in fluid are difficult to describe (Cox, 1970; Shelley and Ueda, 2000). One difficulty arises from the extreme length/width ratio of the filaments, they are extremely thin compared to their length. The fact that the filaments are immersed in a flowing fluid requires a coupling technique (e.g. Cortez et al. (2004)). For the tests at this stage we made the simplification of assuming the fluid to be homogeneous for practical reasons. The homogeneous approach enables using a rather simple and well-known physical description that can be solved using computational mathematics. We hope that this gives us already some insight in the main dependencies of morphology and fluid dynamics. The difference in fluid flow to the fluid containing sperm filaments is a topic for future investigations.

As pointed out in the analyses, these results are not sensitive to our estimates of physical parameters. The qualitative behaviour of the results we found holds even if the true Reynolds number for our system is two orders of magnitude from our estimate which is a rather remote case.

There are at least two areas that should be the subject of future research. First, the fact that we model the fluid homogeneously may be a gross oversimplification because the sperm filaments are very long compared to the duct diameter. We hypothesize that the effect of morphology on the flow rate will increase when the filaments swimming in the fluid are modelled. There are some physical and mathematical challenges linked to this next step that are the subject of ongoing work. Second, to understand the process of sperm transfer, we must first understand the flow of the ejaculate. Only then may we model the spermathecal duct and the spermathecae together and provide a more complete estimate of the influence of morphology on sperm storage.

The flow rate of the seminal fluid is probably strongly related to the number of sperm flowing through the spermathecal duct. Our results show that the irregular duct lining with its increased surface area could allow females increased control over sperm storage. Although such a structure would not allow females to plastically manipulate the conditions of insemination, it could nevertheless provide a larger time window after intromission during which females might influence the number and location of sperm in storage by other means, for example, differential transport via female reproductive tract musculature.

However, because we found the flow rate to be slower in a narrow duct than in the same duct with increased surface area and the same minimum diameter, narrowing the duct would seem to be a more effective (and probably less costly in terms of structural investment) way to slow down sperm movement (Figure 3). Whether the increased surface area has a larger impact on sperm filaments (which might, for example, move with greater or lesser ease through microvilli than a smooth-walled structure) than homogenous fluid is the subject of ongoing work.

Alternatively or additionally, it is possible that the increased surface area is related to an absorptive, secretory function, for example the creation of negative pressure through fluid absorption or the provision of nutrients or spermicidal compounds to the ejaculate.

Evaluating these alternatives will require much more detailed information on the physiology of spermathecal ducts and ideally include empirical observations of the functional significance of increased surface are for sperm movement across females that vary in the morphology of their spermathecal ducts.

Acknowledgements

This work was funded by the University of Zurich, and LFB was supported by the University of Stirling during the preparation of the manuscript. We thank Wolf Blanckenhorn, Marco Demont, Gillian Lye, Andrew Pemberton, Anton Smolianski, and Matthew Tinsley for discussion and helpful comments throughout this study.

References

Arnqvist, G. (2005). *Sexual conflict*. Princetopn University Press.

Arthur, B., Sbilordo, S., Pemberton, A., and Ward, P. (2008). The anatomy of fertilization in the yellow dung fly *Scathophaga stercoraria*. *J. Morphol.*, 269 (5):630–637.

Batchelor, G. (1967). *An Introduction to Fluid Dynamics*. Cambridge Univ. Press.

Bernasconi, G. and Hellriegel, B. (2002). Sperm survival in the female reproductive tract in the fly *Scathophaga stercararia* (L.). *Journal of Insect Physiology*, 48(2):197–203.

Blanckenhorn, W.U., A. B., Meile, P., and Ward, P. (2007). Sexual conflict over copula timing: a mathematical model and a test in the yellow dung fly. *Behav. Ecol.*, 18:958–966.

Ciarlet, P. (1978). *The Finite Element Method for Elliptic Problems*. North Holland, Amsterdam.

Cortez, R., Cowen, N., Dillon, R., and Fauci, L. (2004). Simulation of swimming organisms: Coupling internal mechanics with external fluid dynamics. *Computing in science and engeneering*, 6(3):38–45.

Cox, R. (1970). The motion of long slender bodies in a viscous fluid. 1. general theory. *J. Fluid Mech.*, 44(4):791–810.

Dean, W. (1927). Note on the motion of fluid in a curved pipe. *Phil. Mag.*, 20:208–223.

Dean, W. (1928). Note on the motion of fluid in a curved pipe. *Phil. Mag.*, (7) 5:673–695.

Eberhard, W. (1996). Female control: sexual selection by cryptic female choice. *Princeton University Press, Princeton*, page 501 pp.

Girault, V. and Raviart, P.-A. (1979). *Finite Element Approximation of the Navier-Stokes Equations*. Springer-Verlag, Berlin Heidelberg New York.

Hackbusch, W. (1992). *Elliptic Differential Equations*. Springer Verlag.

Hosken, D., Garner, T., and Ward, P. (2001). Sexual conflict selects for male and female reproductive characters. *Current Biology*, 11:489–493.

Hosken, D., Meyer, E., and Ward, P. (1999). Internal female reproductive anatomy and genital interactions during copula in the yellow dung fly, *Scatophaga stercoraria* (Diptera: Scathophagidae). *Can. J. Zool.*, 77:1975–1983.

Hosken, D. and Ward, P. (2000). Copula in yellow dung flies (scatophaga stercoraria): investigating sperm competition models by histological observation. *Journal of Insect Physiology*, 46:1355–1363.

Lighthill, J. (1975). *Mathematical Biofluiddynamics*. Regional Conference Series in Applied Mathematics, SIAM.

Miller, G. and Pitnick, S. (2002). Sperm-female coevolution in drosophila. *Science*, 298:1230–1233.

Minder, A., Hosken, D., and Ward, P. (2005). Coevolution of male and female reproductive characters across the scatophagidae (diptera). *J. Evol. Biol.*, 18:60–69.

Parker, G. (1970a). Sperm competition and its evolutionary consequences in the insects. *Biol. Rev.*, 45:525–567.

Parker, G. (1970b). Sperm competition and its evolutionary effect on copula duration in the fly *Scatophaga stercoraria*. *J. Insect Physiol.*, 16:1301–1328.

Parker, P. and Simmons, L. (1991). A model of constant random sperm displacement during mating: evidence from *Scatophaga*. *Proc. R. Soc. London Ser. B*, 246:107–115.

Parker, P. and Simmons, L. (1994). Evolution of phenotypic optima and copula duration in dungflies. *Nature*, 370:53–56.

Purcell, E. (1977). Life at low reynolds number. *American Journal of Physics*, 45:3–11.

Schenk, O. and Gärtner, K. (2004). Solving unsymmetric sparse systems of linear equations with pardiso. *Journal of Future Generation Computer Systems*, 20(3):475–487.

Schenk, O. and Gärtner, K. (2006). On fast factorization pivoting methods for symmetric indefinite systems. *Elec. Trans. Numer. Anal.*, 23:158–179.

Shelley, M. and Ueda, T. (2000). The stokesian hydrodynamics of flexing, stretching filaments. *Physica D*, 146:221–245.

Simmons, L., Parker, G., and Stockley, P. (1999). Sperm displacement in the yellow dung fly, *Scatophaga stercoraria*: an investigation of male and female processes. *Am. Nat.*, 153:302–314.

Simmons, L. and Parker, P. (1992). Individual variation in sperm competition success of yellow dung flies, *Scatophaga stercoraria*. *Evolution*, 46(2):366–375.

Simmons, L. and Siva-Jothy, M. (1998). *Sperm competition in insects: mechanismn and potential for selection*. Elselvier Science and Technology.

Ward, P. (2000). Cryptic female choice in the yellow dung fly *Scathophaga stercararia* (L.). *Evolution*, 54(5):1680–1686.

Ward, P. (2007). Postcopulatory selection in the yellow dung fly *Scathophaga stercoraria* (L.) and the mate-now-choose-later mechanism of cryptic female choice. *Advances in the Study of Behavior*, 37:343–369.